CDD*press*

Check for updates

ARTICLE

Flow cytometric single cell-based assay to simultaneously detect cell death, cell cycling, DNA content and cell senescence

Elizabeth Lieschke [1,2], Zilu Wang[1,2], Catherine Chang[1], Clare E. Weeden [1,2], Gemma L. Kelly [1,2,3] and Andreas Strasser [1,2,3 ✉]

Cell death, cell cycle arrest and cellular senescence are three distinct cellular responses that can be induced by oncogene activation and diverse anti-cancer agents, and this often requires the action of the tumour suppressor TP53. Within a cell population, or even within an individual cell, these processes are not necessarily mutually exclusive. It is therefore important to measure all these processes simultaneously. However, current assays generally visualise only one or at best two responses, often only detecting the dominant one. Here, we present a novel flow cytometric assay that allows simultaneous assessment of cell viability and cell cycling through measurement of DNA content and DNA synthesis, and markers of cell senescence at the single cell level. We demonstrate that this assay can be performed on both human and murine cells, that are either cancerous or non-transformed, and can help to dissect complex cell fate decisions. We believe that this experimental tool will be useful for the study of diverse biological processes.

INTRODUCTION

Identifying and measuring distinct cellular responses within a population of cells simultaneously by using a single cell-based assay can provide valuable information for many areas of biomedical research [1, 2]. Cell death [3, 4], cell cycle arrest [5] and cellular senescence [6] are important responses that can be observed in diverse cell types and tissues in vivo and in vitro. The tumour suppressor TP53 can transcriptionally activate all these processes, and additional cellular responses, such as adaptation of metabolism and DNA damage repair [7–9]. Collectively these processes prevent tumour development and expansion [7–9]. TP53 can be activated in response to oncogene activation, many cellular stresses and diverse anti-cancer agents, particularly those that induce DNA damage (e.g. γ-radiation, etoposide) and inhibitors of MDM2 (e.g. nutlin-3a), an E3 ubiquitin ligase that causes ubiquitination of TP53 and thereby primes it for proteasomal degradation [7, 8, 10]. It is important to be able to monitor the different processes induced by TP53 activation in both normal and malignant cells. This can be challenging because within a population of cells, these processes are not necessarily mutually exclusive and evidence suggests that even within a single cell multiple responses can initially be activated, with one process eventually dominating. Most available assays are limited to measuring only one, or at best two, of these processes.

One limitation to looking at these multiple processes simultaneously has been the difficulty in finding a robust marker to detect cellular senescence that is compatible with the methods for assaying the other processes. Recently, urokinase-type plasminogen activator receptor (uPAR) has been shown to be upregulated in a broad range of senescent cells, and in pathologies related to

senescent phenotypes [11–14]. uPAR is a GPI-anchored surface membrane protein that was found to promote motility and invasion of tumour cells through downstream cell signalling [14]. GPI-anchored uPAR can be cleaved from the surface of the plasma membrane and this was reported to be part of the senescence associated secretory phenotype (SASP) [15]. Notably uPAR has been used as a target for senolytic CAR-T cell-based therapies [11].

The inability to measure multiple processes in a single cell leaves many questions unanswered, such as do cells that undergo apoptosis upon TP53 activation also induce the programs for cell cycle arrest and senescence, or in which state of the cell cycle do senescent cells reside? To address these questions, we aimed to develop a flow cytometric assay that can simultaneously measure cell death, cell cycling and cell senescence at the single cell level.

RESULTS

Different cellular responses can be detected within a panel of human cancer-derived cell lines in response to TP53 activation

We selected a panel of nine human cancer-derived cell lines with wild-type (wt) TP53, and as controls, two cancer cell lines that cannot respond to TP53 activating stimuli because they have *TP53* mutations that prevent DNA binding and TP53 target gene induction [7–9]. The selected wt TP53 cancer cell lines represent a diverse range of human cancers, including glioblastoma, osteosarcoma, melanoma, lung carcinoma, breast carcinoma and lymphoma (Table 1), in anticipation that different TP53 activated responses may dominate in different cell types. We used the MDM2 inhibitor nutlin-3a to activate TP53 in a non-genotoxic manner [10], thereby excluding additional stimulation of TP53-

---

Table 1. Characteristics of human cancer-derived cell lines.

Cell line	Cancer type	TP53 status
A549	Lung	wt
H460	Lung	wt
RKO	Colorectal	wt
Lox-IMVI	Melanoma	wt
MCF-7	Breast	wt
U87MG	Glioblastoma	wt
A172	Glioblastoma	wt
SJSA-1	Osteosarcoma	wt
DoHH2	Lymphoma	wt
DLD-1	Colorectal	c.722 C > T p.S241F
Sudhl-4	Lymphoma	c.817 C > T p.R273C

independent processes that may occur and contribute to response after treatment with DNA damage inducing drugs [16]. Compared to treatment with vehicle (DMSO), treatment with nutlin-3a for 72 h induced a 2- to 5-fold increase of TP53 protein in all nine wt TP53 cell lines, as verified by intra-cellular FACS analysis (Fig. 1a). Consistent with previous reports [17], mutant TP53 human cancer cell lines displayed high basal levels of stabilised mutant TP53 protein and exhibited at most only a minor increase in this protein after treatment with nutlin-3a (Fig. 1a).

Upon activation, wt TP53 can induce a range of cellular processes, including apoptotic cell death, cell cycle arrest and cellular senescence. To investigate which TP53 induced outcome occurs in the different human cancer cell lines, we tested their responses to nutlin-3a using individual flow cytometric assays for the detection of apoptosis, cell cycle arrest and cellular senescence. TP53 triggers apoptosis through transcriptional induction of the pro-apoptotic BH3-only proteins PUMA and NOXA [18, 19]. A commonly used flow cytometry-based assay to identify apoptotic cells uses staining with fluorochrome-conjugated annexin-V, which binds to phosphatidylserine residues that are externalised as cells undergo apoptosis. This is combined with the DNA staining dye, propidium iodide (PI), which enters cells when the plasma membrane is no longer intact [20]. Early apoptotic cells are only stained by annexin-V whereas late apoptotic cells (which in culture can undergo so-called secondary necrosis [21]) are stained by both annexin-V and PI. Upon treatment with nutlin-3a, two of the nine wt TP53 cancer cell lines underwent substantial apoptosis (>50% of cells within the population, including early- and late-stage apoptotic cells), with all other wt TP53 cell lines showing <10% death within the population (Fig. 1b; gating shown in Supplementary Fig. S1). Cell lines expressing mutant TP53 did not undergo nutlin-3a-induced apoptosis [10] and provided a negative control for this assay (Fig. 1b).

TP53 induces cell cycle arrest primarily through transcriptional induction of CDKN1A, encoding the cyclin dependent kinase inhibitor p21 (ref. [22]). To detect proliferation arrest and DNA content in the panel of cell lines, we examined BrdU incorporation (4 h pulse) and staining with 7-AAD (7-AminoactinomycinD) 72 h after treatment with nutlin-3a. The proportions of cycling cells (BrdU$^+$ and S phase DNA content) were decreased in all wt TP53 expressing cancer cell lines to <5%. Concordantly, we observed an accumulation of cells in G0/G1 phase, and in some cell lines (e.g. MCF-7 and A549), also an accumulation of cells in G2/M (Fig. 1c; Supplementary Table 1; gating shown in Supplementary Fig. S1).

TP53 can also induce cellular senescence in many solid tumour-derived cell lines [23, 24]. The standard test to detect senescent cells is staining for β-galactosidase, which accumulates in senescent cells, followed by microscopy to detect positively stained cells [25]. Such analysis can be difficult to quantify in an unbiased manner and cannot be readily combined with other read-outs of cell fates. We therefore chose a flow cytometry-based assay using staining with $C_{12}FDG$ as a substrate that yields the fluorochrome FITC upon processing by β-galactosidase (SA β-gal) [26]. In agreement with findings from others using this method [27–29], we observed that the results from this assay correlated well with the standard microscopy-based SA β-gal staining (Supplementary Fig. S2a). Using this flow cytometry-based assay, we found that upon treatment with nutlin-3a for 72 h, the wt TP53 cancer cell lines that did not undergo considerable apoptosis demonstrated substantially increased SA β-gal staining, albeit to varying extents (~20–60%; Fig. 1d; gating shown in Supplementary Fig. S1). As expected [10], the mutant TP53 cancer cell line did not show evidence of cellular senescence following treatment with nutlin-3a (Fig. 1d). Moreover, CRISPR-mediated deletion of wt TP53 prevented nutlin-3a induced induction of senescence in the HCT116 and A549 cancer cell lines (Supplementary Fig. S3).

TP53 can simultaneously activate multiple processes in the same cell line

These results demonstrate accurate detection of multiple cell fates using individual flow cytometry-based assays. Yet performing multiple assays to detect the different responses individually is time consuming, expensive, impractical when cell numbers are limited, and presents a significant challenge for deducing an overall picture of all the processes activated within an individual cell or a complex cell population. Therefore, we aimed to establish a single flow cytometry-based assay that could simultaneously detect all three outcomes, namely cell death, cell cycle arrest and senescence. As a starting point we adapted the individual assays and selected four wt TP53 cell lines: two cell lines that mainly undergo apoptosis (DoHH2 and SJSA-1) and two cell lines that mainly undergo cell cycle arrest and senescence (RKO and H460) upon treatment with nutlin-3a. All wt TP53 cancer cell lines chosen for these experiments displayed statistically significant increases in TP53 protein after nutlin-3a treatment, except SJSA-1 (Fig. 1a). Despite only modest and variable increases of TP53 in SJSA-1 cells, this line showed consistent apoptotic death upon nutlin-3a treatment, and hence was also chosen for these studies. As a non-responding control, we used DLD-1 cells which express mutant TP53.

Measuring SA β-galactosidase activity was not possible in the combined assay, because it is not compatible with the fixation needed to detect BrdU incorporated into the DNA of proliferating cells. Instead, we opted to stain with an antibody to detect uPAR/CD87. We confirmed in the human lung carcinoma cell line, H460, that SA β-gal staining and uPAR staining detected comparable numbers of cells undergoing senescence (Supplementary Fig. S2b). To confirm that the same cells in the population were expressing both uPAR and β-gal, we treated the human lung carcinoma line A549 with for 72 h with nutlin-3a or DMSO (vehicle control). We then stained for uPAR and sorted the lowly as well as the highly uPAR expressing cells. These cell fractions were then fixed and stained for β-gal. This confirmed that the high uPAR expressing cells also expressed the highest levels of SA β-gal (Supplementary Fig. S4).

Using murine dermal fibroblasts (MDFs) and the human cancer cell lines HCT116 and A549, we also found that the increase in uPAR expression was detectable at both the surface level by staining unfixed cells and the total level within cells by staining fixed cells (Supplementary Fig. S5). This indicates that this marker can be used as a surface stain to detect upregulation of uPAR as a marker of senescent cells.

In the combined assay for simultaneous detection of cell death, cell cycling, DNA content and cell senescence, the H460 and RKO cells demonstrated increased uPAR staining after treatment with nutlin-3a (Fig. 2a; gating shown in Supplementary Fig. S1).
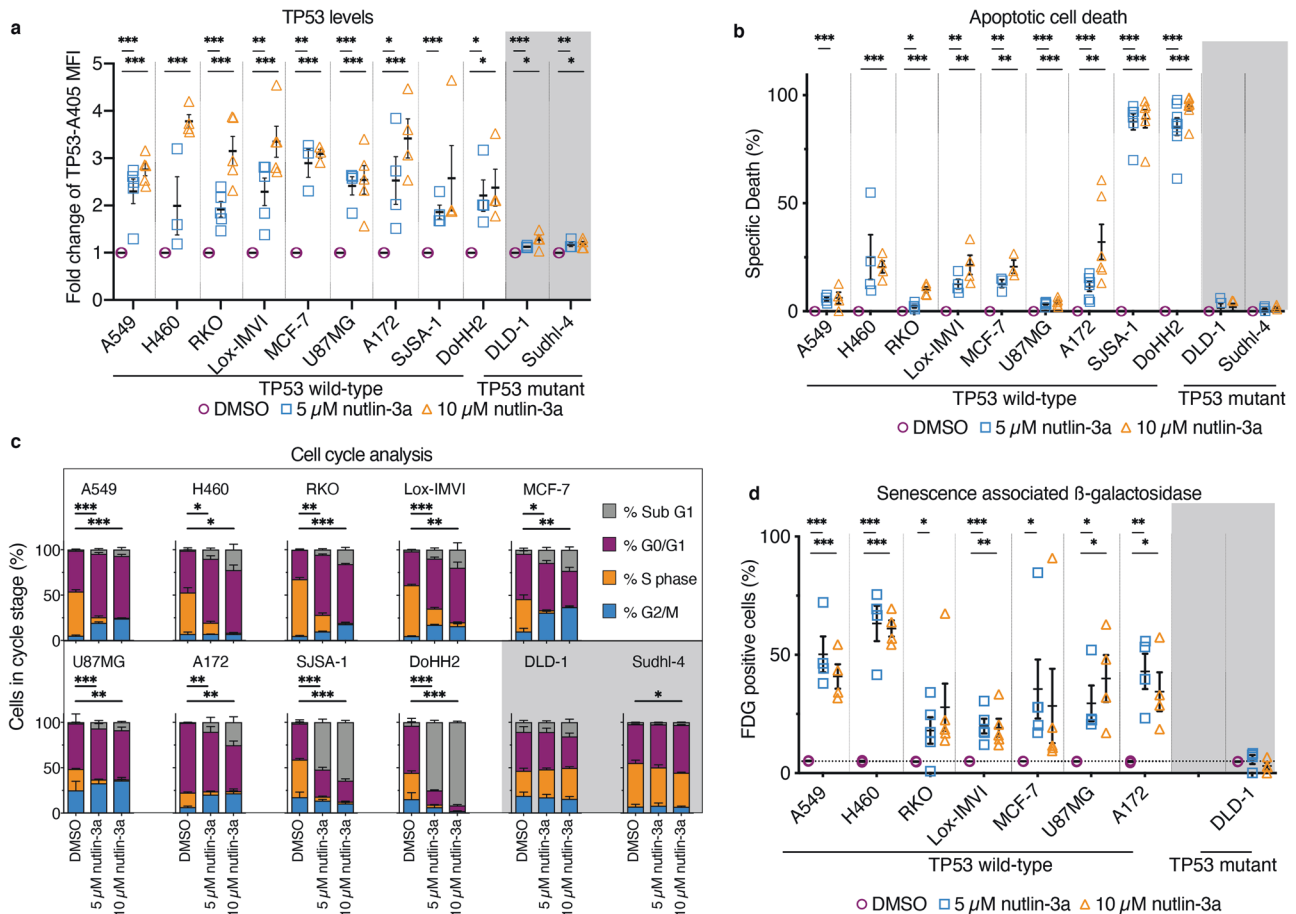
Fig. 1 Response of diverse human cancer-derived cell lines to TP53 activation using standard flow cytometry-based methods. a TP53 protein levels were measured by flow cytometry as a read-out of TP53 activation following 72 h of treatment with the indicated concentration of nutlin-3a. The fold induction relative to DMSO treated cells is plotted; $n = 3–5$. **b** Apoptotic cell death was detected by staining cells with annexin-V-FITC and PI at 72 h after treatment with the indicated concentration of nutlin-3a or DMSO (control). Drug-induced cell death relative to DMSO treatment is shown. $n = 3–8$. **c** Cell cycle analysis was performed following 72 h treatment with DMSO (control) or the indicated concentration of nutlin-3a by pulsing cells for the last 4 h of treatment with BrdU, which is incorporated into newly synthesised DNA. The cells were then fixed, permeabilised and stained with antibodies against BrdU plus the DNA stain, 7-AAD, followed by flow cytometric analysis. Changes in S phase indicated by bar. See Supplementary Table 1 for full statistical comparisons. $n = 3–5$. **d** Cellular senescence was detected following 72 h treatment with the indicated concentration of nutlin-3a or DMSO (control) by flow cytometry after incubating cells with a substrate for β-galactosidase ($C_{12}FDG$) that produces the fluorochrome FITC. $n = 4–5$. DLD-1 cells, and in (**a**–**c**) also Sudhl-4 cells, both of which express mutant TP53, were included as non-responding controls. In (**a**–**d**), mean ± SEM is plotted, $p = *\leq 0.05$, **$\leq$ 0.01, ***$\leq$ 0.001. In (**a**, **b** and **d**), p values are calculated using t tests corrected for multiple comparisons. In (**c**), p values are calculated by 2-way ANOVA, corrected for multiple comparisons using Dunnett's correction. In (**a**, **b** and **d**) each symbol represents data from an individual experiment.

Interestingly, we were able to detect an increase in uPAR staining in SJSA-1 cells, which we had not previously been able to assess by SA β-gal staining in the individual assays, due to the large proportion of these cells undergoing apoptosis upon treatment with nutlin-3a (Fig. 2a). In the cell lines in which both types of assays to detect senescent cells were performed, there were only small differences in the extent of uPAR staining compared with SA β-gal activity. These differences could be due to these markers being expressed slightly differently in populations of senescent cells, or that we include a sub-G1 DNA content (dying/dead) cell population in the combined assay, which had usually been excluded due to limitations of the previously used individual assays.

When looking at cell populations as a whole, these five cell lines underwent the same processes to a similar extent as seen in the single assays (Fig. 2a–c; gating shown in Supplementary Fig. S1). For SJSA-1 and DoHH2 cells, ~80% of cells stained positive for annexin-V (Fig. 2b), indicating they were undergoing apoptosis. Interestingly, with the added information from the cell cycle

analysis incorporated in the combined assay, we can see that annexin-V positive cells not only resided in the sub-G1 DNA content population, as expected, but also included cells residing in the G0/G1 phase (Fig. 3a).

All five cell lines tested showed similar cell cycle profiles when using the combined cell fate assay compared to the single assays, with a marked decrease in S phase cells observed after 72 h treatment with nutlin-3a, and an increase in cells in the G0/G1 stage in RKO and H460 cells (Fig. 2c). Additionally, we can see that uPAR positive senescent cells reside in both G0/G1 and G2/M stages of the cell cycle, but not in the sub-G1 population (Fig. 3b). This is consistent with reports that TP53 activation can induce cell cycle arrest and entry into senescence at both the G1/S and G2/M boundaries [5].

Murine dermal fibroblasts can undergo apoptosis, cell cycle arrest, and senescence after TRP53 activation
To confirm the versatility of this combined assay, we also applied it to the study of murine dermal fibroblasts (MDF), which after
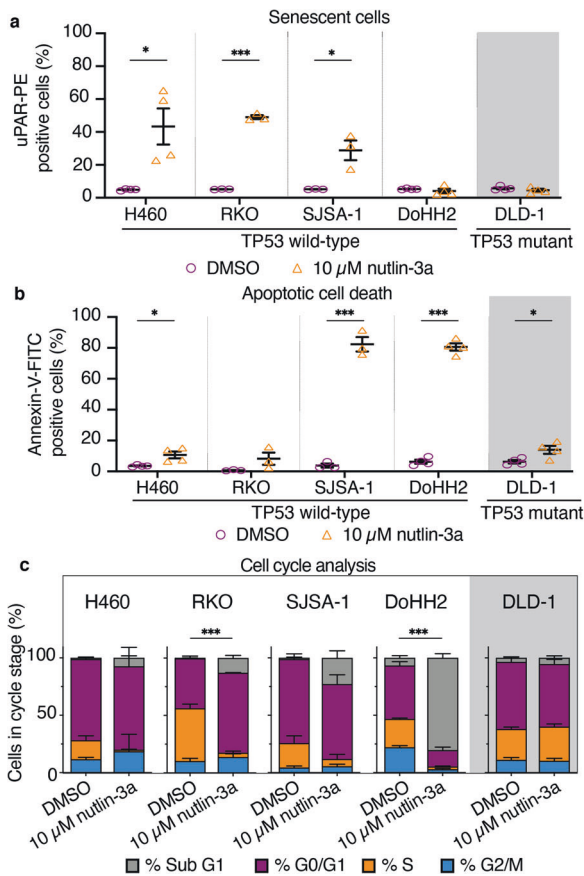
Fig. 2 Response of diverse human cancer-derived cell lines to TP53 activation after treatment for 72 h with 10 μM nutlin-3a using a novel combined flow cytometry-based method. **a** Percentages of cells stained for uPAR as an indication of cellular senescence. **b** Percentages of cells stained with annexin-V-FITC as an indicator of apoptosis. **c** Percentages of cells in the different stages of the cell cycle – DNA content: sub-G1 DNA content (dying), G0 and G1, S, or G2 and M, using staining for BrdU incorporation and DNA content (DAPI). DLD-1 cells, which express mutant TP53, were included as a non-responding control. $n = 3$–4, mean ± SEM plotted, $p =$ *≤ 0.05, **≤ 0.01, ***≤ 0.001. In (**a**, **b**), p values were determined by t tests corrected for multiple comparisons. In (**c**), p value was calculated by 2-way ANOVA correct for multiple comparisons using Sidak's test. For full statistical comparisons, see Supplementary Table 2. In (**a** and **b**), each symbol represents data from an individual experiment.

TRP53 (the nomenclature for the murine protein) activation are reported to undergo cell cycle arrest and cellular senescence [30]. We utilised nutlin-3a to activate TRP53 in a non-genotoxic manner and in addition, we also treated these cells with the DNA damaging agent etoposide, to induce TRP53 activation, albeit alongside additional processes. Using uPAR staining (Fig. 4a), we could see that treatment with nutlin-3a induced senescence in wt $Trp53$ MDFs, but not in $Trp53^{-/-}$ control MDFs. Of note, treatment with etoposide caused a marked increase in uPAR staining not only in wt $Trp53$ MDFs but also in $Trp53^{-/-}$ MDFs. This is consistent with the notion that DNA damage inducing drugs can induce cell growth inhibitory responses not only through TP53/TRP53-dependent processes but also through processes that are independent of this tumour suppressor [16, 31–33].

A small increase in apoptotic cell death, as detected by annexin-V plus DAPI staining, was seen after treatment with nutlin-3a only in the wt MDFs, whereas etoposide treatment induced apoptosis in both wt as well as $Trp53^{-/-}$ MDFs (Fig. 4b).

Combined DNA content and BrdU staining showed that treatment with nutlin-3a and etoposide both decreased the proportions of cycling (S phase) cells in wt MDFs. Only treatment with etoposide, but as expected not addition of nutlin-3a, caused a decrease in cells residing in S phase in $Trp53^{-/-}$ MDFs. In wt MDFs, nutlin-3a treatment caused an increase in the proportions of cells in the G0/G1 state, whereas exposure to etoposide increased the proportions of these cells in the G2/M state at 24 h, before progressing to substantial cell death at 72 h (sub-G1 DNA content state) (Fig. 4c).

As we saw in the human cancer-derived cell lines, we observed that annexin-V positive cells could reside not only in the sub-G1 DNA content state but also the G0/G1 state (Fig. 5a). Conversely, uPAR positive cells resided in the G0/G1 and G2/M states but not in the sub-G1 DNA content population (Fig. 5b).

Additionally, we observed in MDFs treated with nutlin-3a or etoposide, that there was a population of annexin-V positive cells that were also uPAR positive, indicating that these cells were inducing both of the apoptosis and senescence programs (Fig. 6a, b).

Collectively, these findings show that our novel flow cytometric single cell-based assay for the detection of DNA content, DNA synthesis, cell senescence and apoptotic cell death can be readily adapted for use in murine cells (and if suitable antibodies to uPAR are available, also to cells from other species).

DISCUSSION

We have developed a simple, cheap, and robust combined flow cytometry-based assay to simultaneously examine and quantify the different predominate fates of cells after TP53 activation: cell cycle arrest, entry into cellular senescence and apoptotic cell death. This assay saves both time and resources whilst reliably reproducing the results seen when these assays are carried out individually. We have demonstrated its validity in both human and murine cells after TP53/TRP53 activation, with our results correlating well with previous studies [30, 34–36]. This assay has the potential to be used in the analysis of diverse biological processes, including to detect responses of cell populations driven by TP53-independent stimuli, such as cancer treatments including glucocorticoids [16].

Finding a robust marker of cell senescence that can be seen across multiple cell types and staining for which is compatible with other staining techniques has been a limiting factor in the field. The traditional methods using examination of senescence associated β-galactosidase either by microscopy or by flow cytometry, or looking at morphological changes [37], has been restrictive due to the need to be performed separately from other assays, such as analysis of DNA synthesis. Other markers of cellular senescence, such as factors in the SASP (e.g. IL-6) (ref. [38]), are only produced by a fraction of senescent cells, and therefore are not reliable for a combined assay. Moreover, these factors are released from cells and therefore can only be detected by treating cells with protein export inhibitors that may impact other cellular processes measured in a combined cell fate assay. Flow cytometric analysis of the surface markers B2MG and DEP1 has been used to detect senescent bladder cancer cells [39], but the applicability to other cell types has not been validated. We have shown here that uPAR, which was previously shown to be a marker of cellular senescence in lung cancer models and hepatocytes [11], can also be applied across other cell types, such as colorectal cancers and murine fibroblasts, making this an informative and versatile marker of this cell fate. The biological reason for the upregulation of uPAR in senescent cells is not clear although it is known that uPAR expression is increased in response to diverse stresses, immune responses and inflammation [40]. The conditions that induce cell senescence also cause these responses, and this might be a reason for this increase in uPAR.
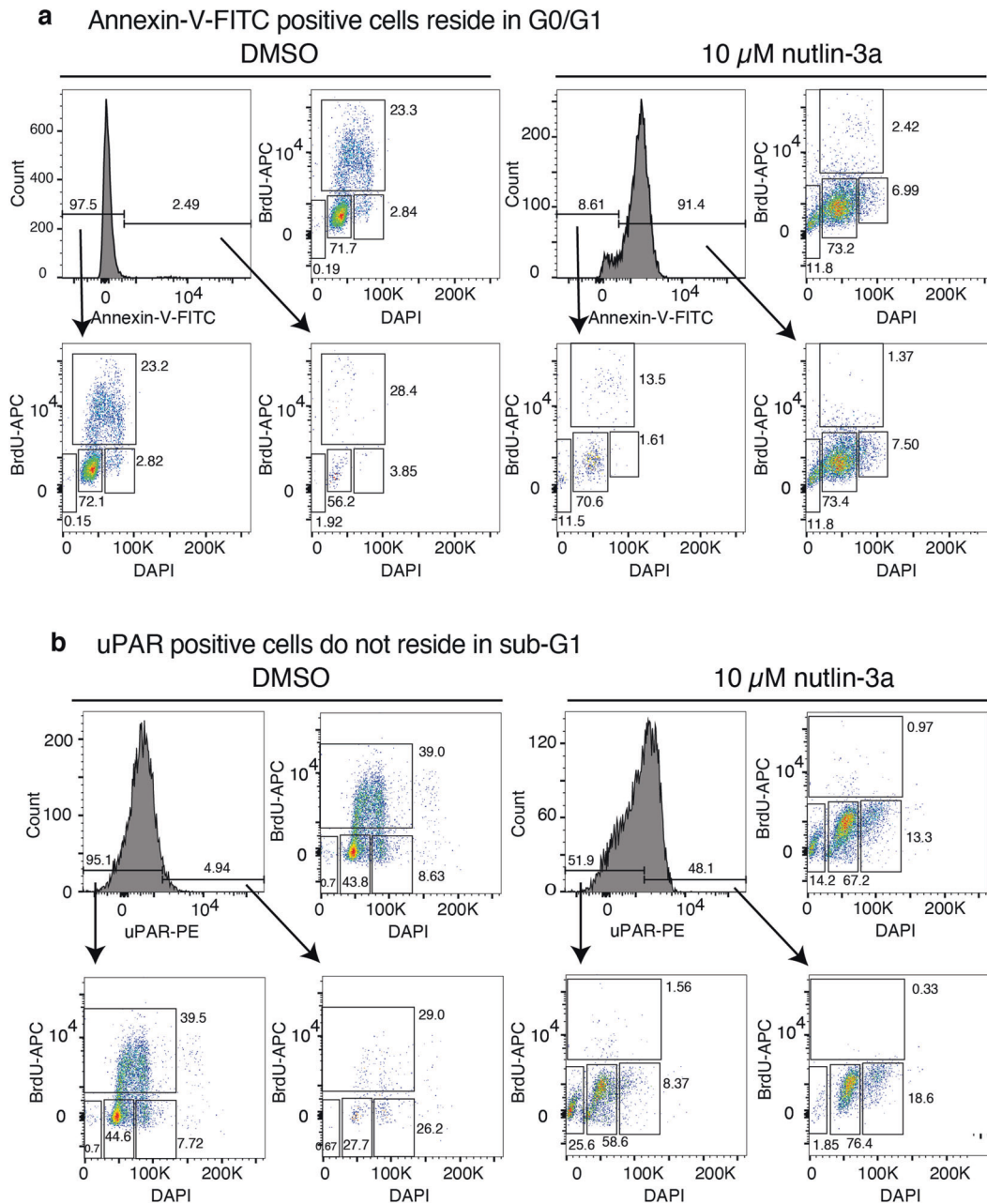
Fig. 3 Annexin-V positive cells and uPAR positive cells can reside in different cell cycle stages. a Annexin-V-FITC positive cells reside in the G0/G1 as well as the sub-G1 DNA content states. Flow cytometry histogram of SJSA-1 cells that had been treated for 72 h with 10 μM nutlin-3a or DMSO (control) and were then stained with annexin-V-FITC plus DAPI to reveal surface exposed phosphatidylserine and DNA content, respectively. The annexin-V-FITC negative nutlin-3a treated cells have a similar cell cycle distribution as the entire population of DMSO treated (control) cells, whereas the annexin-V-FITC positive cells reside in the G0/G1 and sub-G1 DNA content (dying cells) states. **b** uPAR positive cells reside in the G0/G1 and the G2/M stages of the cell cycle, but not in the sub-G1 (dying/dead) population state. Flow cytometry histogram of RKO cells that had been treated for 72 h with 10 μM nutlin-3a or DMSO (control) and then stained with an antibody against uPAR conjugated to PE plus DAPI to reveal senescent cells and DNA content, respectively.

Most importantly, this combined assay has already allowed us to make discoveries that are not possible in the single assays, such as the observation that upon TP53 activation cells can simultaneously activate the programs for apoptosis, cell cycle arrest and cell senescence, although cell death will dominate. Moreover, our new assay revealed that upon TRP53/TP53 activation apoptotic cells can be found not only as expected in the sub-G1 DNA content state, but also in G1, and that senescent cells reside in the G0/G1 and G2/M cell cycle phases but not in the S phase. We predict that this new assay will enhance the analysis of many complex cellular responses and thereby provide interesting new insight into diverse biological processes.

MATERIALS AND METHODS
Cell lines and cell culture conditions
Human cancer-derived cell lines (A172, H460, A549, RKO, DLD-1, Lox-IMVI, MCF-7, DoHH2, Sudhl-4, SJSA-1, U87MG and HCT116) were cultured as described in the Supplementary Methods. All cell lines used were routinely tested for mycoplasma contamination using the Lonza kit according to the manufacturer's instructions.
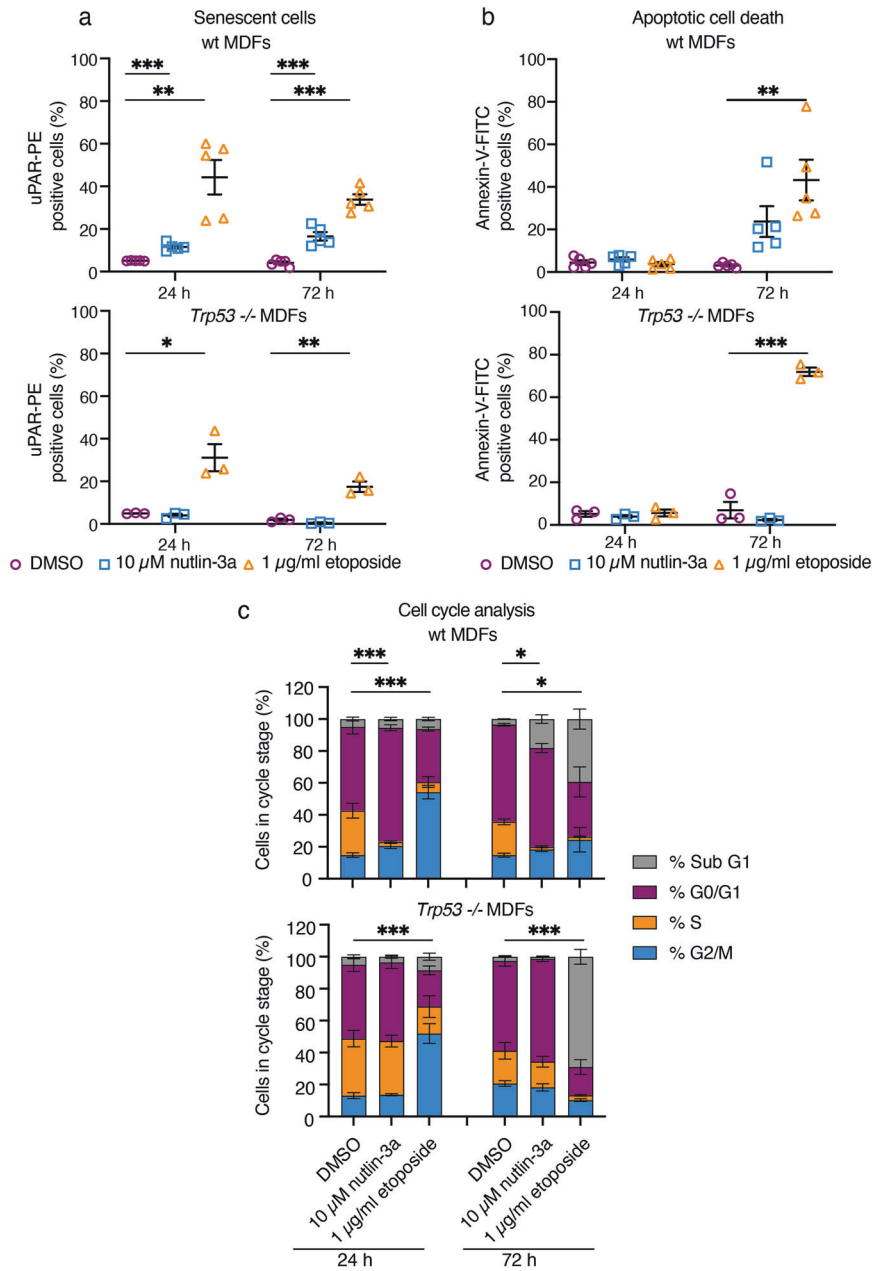
Fig. 4 Response of murine dermal fibroblasts (MDFs) to 10 μM nutlin-3a or 1 μg/mL etoposide after 24 h and 72 h. a Percentages of MDFs stained for uPAR as an indicator of cellular senescence. **b** Percentages of MDFs stained with annexin-V-FITC as an indicator of apoptosis. **c** Percentages of MDFs in the difference stages of the cell cycle – DNA content: sub-G1 DNA content (dying), G0 and G1, S, or G2 and M, using staining for BrdU incorporation and DNA content (DAPI). $n = 3$–5, mean ± SEM plotted, $p = *≤0.05$, $**≤0.01$, $***≤0.001$. In (**a**, **b**), p values were determined by t tests corrected for multiple comparisons. In (**c**), p values were calculated by 2-way ANOVA correct for multiple comparisons using Sidak's test. For full statistical comparisons, see Supplementary Table 3. In (**a** and **b**), each symbol represents data from an individual experiment.

Cell line authentication

All human cancer-derived cell lines were authenticated by short tandem repeat (STR) profiling. DNA was extracted using the DNeasy Blood and Tissue kit (Qiagen #69506) as per the manufacturer's instructions and sent to the Australian Genome Research Facility (AGRF) for GenePrint 10 cell line authentication. Sequencing to confirm *TP53* status was performed as described in the Supplementary Methods.

Mice

All animal experiments were conducted with the approval of the WEHI Animal Ethics Committee following the guidelines set out by the National Health and Medical Research Council (NHMRC). *Trp53*$^{-/-}$ mice have been previously described [41] and have been backcrossed to C57BL/6 mice for 20 generations prior to use in these experiments.

Murine dermal fibroblast (MDF) generation and culture conditions

MDFs were generated from tails of 8–12 week-old wt or *Trp53*$^{-/-}$ mice. Bone was removed from skin and the skin was then digested in 2.1 U/mL dispase II (Sigma–Aldrich #D4693) in DMEM (Gibco #11885-092) at 4 °C overnight. The dermis was peeled from the epidermis and placed in Collagenase IV 0.42 mg/mL (Sigma–Aldrich #C5138) in DMEM at 37 °C for 1 h. The dermis was passed through a 100 μm mesh, and collagenase washed away with DMEM. Cells were then plated and cultured in DMEM + 10% Heat Inactivated-FBS at 37 °C in 5% CO_2 and used for assays on passages 1–3.
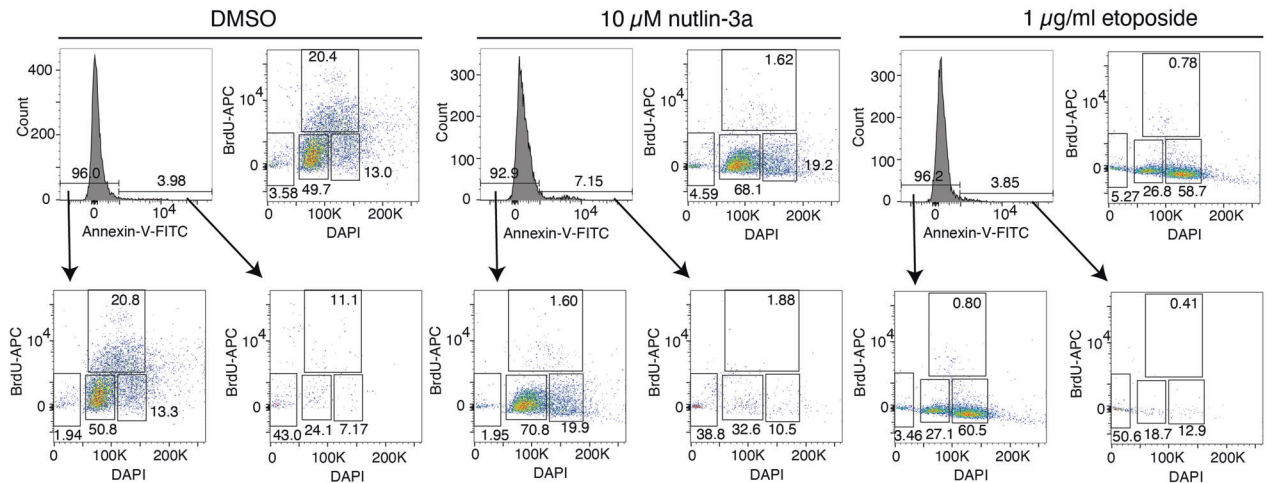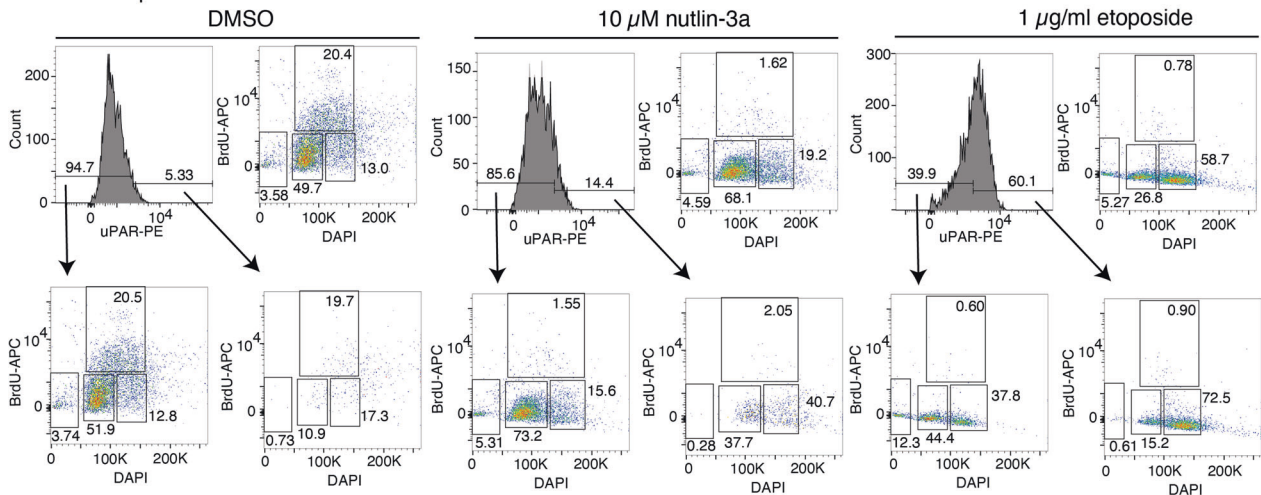
Fig. 5 A novel combined flow cytometric single cell-based assay for the simultaneaous detection of cell cycling, cell senescence and apoptotic cell death in mouse dermal fibroblasts (MDFs). a Annexin-V-FITC positive cells reside in the G0/G1 as well as the sub-G1 DNA content state. Flow cytometry histogram of MDFs that had been treated for 24 h with 10 μM nutlin-3a, 1 μg/mL etoposide or DMSO (control) and were then stained with annexin-V-FITC plus DAPI to reveal surface exposed phosphatidylserine and DNA content, respectively. The annexin-V-FITC negative nutlin-3a treated cells have a similar cell cycle distribution as the entire population of DMSO treated (control) cells, whereas the annexin-V-FITC positive cells reside in the G0/G1 and sub-G1 (dying cells) states. **b** uPAR positive cells reside in the G0/G1 and the G2/M stages of the cell cycle, but not the sub-G1 (dying/dead) cell population. Flow cytometry histogram of MDFs that had been treated for 24 h with 10 μM nutlin-3a, 1 μg/mL etoposide or DMSO (control) and then stained with an antibody against uPAR conjugated to PE plus DAPI to reveal senescent cells and DNA content, respectively.

Flow cytometry assays

Adherent cell lines or MDFs were plated and left to settle for 24 h in an incubator with either 5% or 10% CO_2 at 37 °C. Medium was replaced with medium containing nutlin-3a (5 μM or 10 μM, Cayman Chemicals #18585), etoposide (1 μg/mL, Ebewe Interpharma) or DMSO (vehicle control) and cells incubated for 24 or 72 h. Suspension cells were plated out immediately before addition of drug or DMSO. At the time for analysis, suspension cells were transferred into a round bottomed plate. Adherent cells were dissociated with trypsin (Sigma #T4174), keeping both the supernatant and the trypsinised fractions for analysis. Cells were then centrifuged to remove medium and resuspended as specified below for the flow cytometric assay to be performed.

Detection of TP53 protein by intracellular flow cytometric analysis

Cells were resuspended and stained using the LIVE/DEAD fixable far red dead cell staining kit (Invitrogen #L10120) for 30 min before fixing and permeabilising with the Foxp3/Transcription Factor Staining buffer set (Affymetrix eBioscience #00-5523). Cells were stained with A405-conjugated TP53 antibody (clone FL-393, Santa Cruz), washed and analysed on an LSRIIW or Fortessa flow cytometer.

Flow cytometric analysis for senescence associated β-galactosidase

Before cells were harvested, medium was removed from culture wells and replaced with medium containing 100 nM bafilomycin A1 (Sigma–Aldrich #B1793) and 5 μM or 10 μM nutlin-3a or DMSO (vehicle control). Cells were incubated for an additional 1 h. 33 μM C_{12}FDG (Invitrogen #D2893) was then added and cells incubated for a further 2 h. Cells were then harvested as described above and resuspended in PBS contain 1 μg/mL DAPI (Sigma D9542). Cells were analysed immediately on an LSRIIC flow cytometer.

Flow cytometric analysis for apoptotic cell death

Cells were resuspended in 50–100 μL annexin-V binding buffer (0.1 M Hepes pH 7.4, 1.4 M NaCl, 25 mM $CaCl_2$) containing annexin-V-FITC (Biolegend #640905) and PI 1 μg/mL. Cells were then analysed on an LSR or Fortessa flow cytometer (Becton Dickinson).
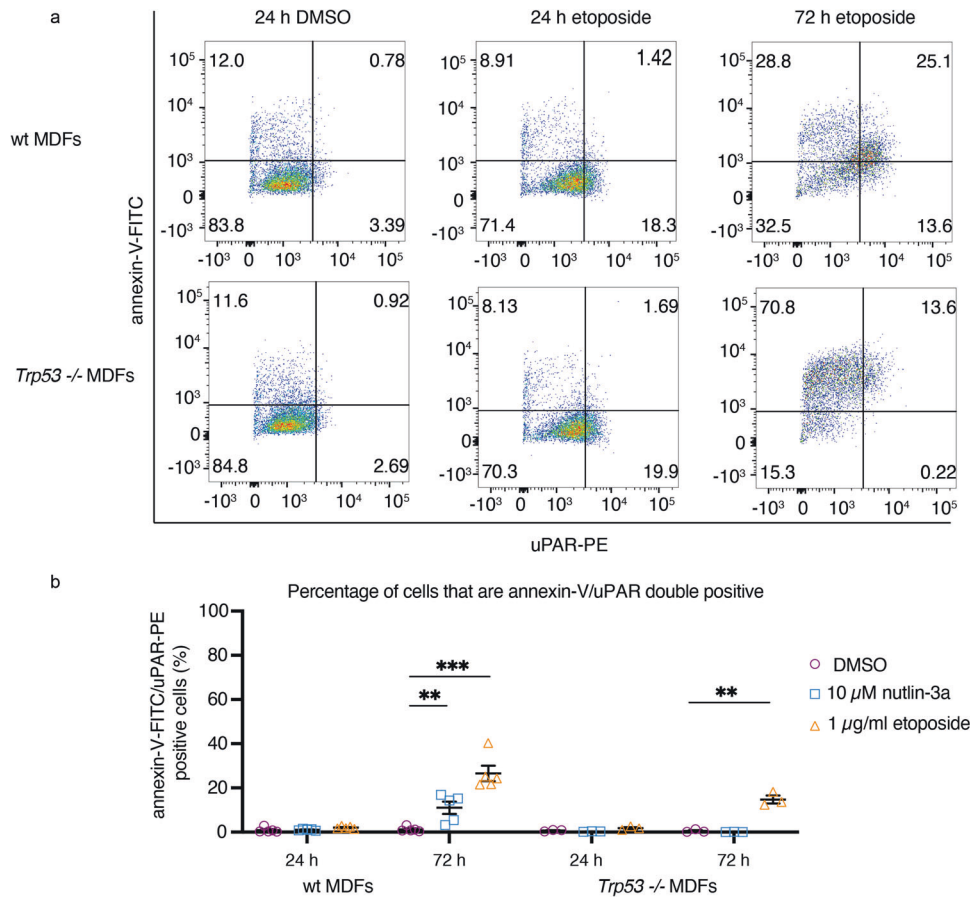
Fig. 6 Individual cells can activate several cell fate determining processes simultaneously. a Flow cytometry dot plots of wt and $Trp53^{-/-}$ MDFs after 24 h DMSO (control), or 24 h or 72 h treatment with 1 μg/mL etoposide. Cells were subjected to the combined cell fate determining flow cytometric assay (see Fig. 5 and Materials and Methods). Annexin-V-FITC/uPAR-PE double positive cells can be seen at 72 h in etoposide treated MDFs of both genotypes. Representative example of $n = 3–5$ experiments. **b** Combined graph of data from all experiments using either treatment with DMSO (control), 1 μg/mL etoposide or 10 μM nutlin-3a for 24 or 72 h. Each symbol represents data from MDFs from an individual mouse. $n = 3–5$, mean ± SEM plotted, $p = *≤0.05$, $**≤0.01$, $***≤0.001$. p values were determined by t tests corrected for multiple comparisons.

Flow cytometry-based cell cycle analysis

At 4 h before harvesting for analysis, cells were pulsed with BrdU (3 μg/mL). Cells were harvested as described above, then fixed and stained using the APC BrdU Flow kit (BD Pharmingen™ #557892) following the manufacturer's protocol. DNA was loosened by treatment with 0.025 mg/mL (50 U) DNAse (Worthington LS002140) in 0.15 M NaCl, 42 mM MgCl₂ in PBS for 15 min at 37 °C, or alternatively using the APC BrdU Flow kit protocol. Cells were resuspended in BD permeabilisation/wash buffer with 7-AAD (2.5 μg/mL). Samples were analysed within 24 h on the LSR IIW (Becton Dickinson) at a flow rate of <400 events/sec.

Combined flow cytometry-based assay to simultaneously detect cell death, cell cycling, DNA content and cell senescence

BrdU (3 μg/mL; BD kit) was added to the culture medium 4 h before the cells were harvested as described above. Cells were stained for 30 min on ice in 100 μL annexin-V binding buffer (0.1 M Hepes pH 7.4, 1.4 M NaCl, 25 mM CaCl₂) containing annexin-V-FITC (Biolegend #640945). Cells were then washed and fixed using the APC BrdU Flow kit (BD Pharmingen™ #557892), stained with an antibody against BrdU conjugated to APC and an antibody against uPAR conjugated to PE (human uPAR, BioLegend #338906, clone VIM5; mouse uPAR, R&D Systems #FAB531P, clone 109801) before being resuspended in PBS containing 10% FBS DAPI (1 μg/mL) and analysed on an LSRIIW or BD Symphony flow cytometer (Becton Dickinson) at a flow rate of less than 400 events/second.

SA β-gal staining

SA β-gal staining was performed as previously described [25].

DATA AVAILABILITY

All data will be made available on request.

REFERENCES

1. Sarrion-Perdigones A, Chang L, Gonzalez Y, Gallego-Flores T, Young DW, Venken KJT. Examining multiple cellular pathways at once using multiplex hextuple luciferase assaying. Nat Commun. 2019;10:5710.
2. Garvey CM, Spiller E, Lindsay D, Chiang CT, Choi NC, Agus DB, et al. A high-content image-based method for quantitatively studying context-dependent cell population dynamics. Sci Rep. 2016;6:29752.
3. Bedoui S, Herold MJ, Strasser A. Emerging connectivity of programmed cell death pathways and its physiological implications. Nat Rev Mol Cell Biol. 2020;21:678–95.
4. Green DR. The coming decade of cell death research: five riddles. Cell. 2019;177:1094–107.
5. Otto T, Sicinski P. Cell cycle proteins as promising targets in cancer therapy. Nat Rev Cancer. 2017;17:93–115.
6. Gorgoulis V, Adams PD, Alimonti A, Bennett DC, Bischof O, Bishop C, et al. Cellular senescence: defining a path forward. Cell. 2019;179:813–27.
7. Vousden KH, Lane DP. p53 in health and disease. Nat Rev Mol Cell Biol. 2007;8:275–83.

8. Kastenhuber ER, Lowe SW. Putting p53 in Context. Cell. 2017;170:1062–78.

9. Janic A, Valente LJ, Wakefield MJ, Di Stefano L, Milla L, Wilcox S, et al. DNA repair processes are critical mediators of p53-dependent tumor suppression. Nat Med. 2018;24:947–53.

10. Vassilev LT, Vu BT, Graves B, Carvajal D, Podlaski F, Filipovic Z, et al. In vivo activation of the p53 pathway by small-molecule antagonists of MDM2. Science. 2004;303:844–8.

11. Amor C, Feucht J, Leibold J, Ho YJ, Zhu C, Alonso-Curbelo D, et al. Senolytic CAR T cells reverse senescence-associated pathologies. Nature. 2020;583:127–32.

12. Simon DI, Rao NK, Xu H, Wei Y, Majdic O, Ronne E, et al. Mac-1 (CD11b/CD18) and the urokinase receptor (CD87) form a functional unit on monocytic cells. Blood. 1996;88:3185–94.

13. Hayek SS, Sever S, Ko YA, Trachtman H, Awad M, Wadhwani S, et al. Soluble urokinase receptor and chronic kidney disease. N Engl J Med. 2015;373:1916–25.

14. Smith HW, Marshall CJ. Regulation of cell signalling by uPAR. Nat Rev Mol Cell Biol. 2010;11:23–36.

15. Coppe JP, Patil CK, Rodier F, Sun Y, Munoz DP, Goldstein J, et al. Senescence-associated secretory phenotypes reveal cell-nonautonomous functions of oncogenic RAS and the p53 tumor suppressor. PLoS Biol. 2008;6:2853–68.

16. Strasser A, Harris AW, Jacks T, Cory S. DNA damage can induce apoptosis in proliferating lymphoid cells via p53-independent mechanisms inhibitable by Bcl-2. Cell. 1994;79:329–39.

17. Aubrey BJ, Janic A, Chen Y, Chang C, Lieschke EC, Diepstraten ST, et al. Mutant TRP53 exerts a target gene-selective dominant-negative effect to drive tumor development. Genes Dev. 2018;32:1420–9.

18. Villunger A, Michalak EM, Coultas L, Mullauer F, Bock G, Ausserlechner MJ, et al. p53- and drug-induced apoptotic responses mediated by BH3-only proteins puma and noxa. Science. 2003;302:1036–8.

19. Oda E, Ohki R, Murasawa H, Nemoto J, Shibue T, Yamashita T, et al. Noxa, a BH3-only member of the Bcl-2 family and candidate mediator of p53-induced apoptosis. Science. 2000;288:1053–8.

20. Vermes I, Haanen C, Steffens-Nakken H, Reutelingsperger C. A novel assay for apoptosis. Flow cytometric detection of phosphatidylserine expression on early apoptotic cells using fluorescein labelled Annexin V. J Immunol Methods. 1995;184:39–51.

21. Wyllie AH, Kerr JF, Currie AR. Cell death: the significance of apoptosis. Int Rev Cytol. 1980;68:251–306.

22. Harper JW, Adami GR, Wei N, Keyomarsi K, Elledge SJ. The p21 Cdk-interacting protein Cip1 is a potent inhibitor of G1 cyclin-dependent kinases. Cell. 1993;75:805–16.

23. Wang B, Kohli J, Demaria M. Senescent cells in cancer therapy: friends or foes? Trends Cancer. 2020;6:838–57.

24. Tonnessen-Murray CA, Lozano G, Jackson JG. The regulation of cellular functions by the p53 protein: cellular senescence. Cold Spring Harb Perspect Med. 2017;7: a026112.

25. Dimri GP, Lee X, Basile G, Acosta M, Scott G, Roskelley C, et al. A biomarker that identifies senescent human cells in culture and in aging skin in vivo. Proc Natl Acad Sci USA. 1995;92:9363–7.

26. Plovins A, Alvarez AM, Ibanez M, Molina M, Nombela C. Use of fluorescein-di-beta-D-galactopyranoside (FDG) and C12-FDG as substrates for beta-galactosidase detection by flow cytometry in animal, bacterial, and yeast cells. Appl Environ Microbiol. 1994;60:4638–41.

27. Cahu J, Sola B. A sensitive method to quantify senescent cancer cells. J Vis Exp. 2013;78:e50494.

28. Fiering SN, Roederer M, Nolan GP, Micklem DR, Parks DR, Herzenberg LA. Improved FACS-Gal: flow cytometric analysis and sorting of viable eukaryotic cells expressing reporter gene constructs. Cytometry. 1991;12:291–301.

29. Fiering S. FACS-Gal: Flow Cytometric Assay of β-galactosidase in Viable Cells. In: Diamond RA, Demaggio S, editors. In Living Color: Protocols in Flow Cytometry and Cell Sorting. Berlin, Heidelberg: Springer Berlin Heidelberg; 2000. p. 227–58.

30. Attardi LD, de Vries A, Jacks T. Activation of the p53-dependent G1 checkpoint response in mouse embryo fibroblasts depends on the specific DNA damage inducer. Oncogene. 2004;23:973–80.

31. Jacobs JJ, de Lange T. Significant role for p16INK4a in p53-independent telomere-directed senescence. Curr Biol. 2004;14:2302–8.

32. Zhu J, Woods D, McMahon M, Bishop JM. Senescence of human fibroblasts induced by oncogenic Raf. Genes Dev. 1998;12:2997–3007.

33. Probin V, Wang Y, Bai A, Zhou D. Busulfan selectively induces cellular senescence but not apoptosis in WI38 fibroblasts via a p53-independent but extracellular signal-regulated kinase-p38 mitogen-activated protein kinase-dependent mechanism. J Pharm Exp Ther. 2006;319:551–60.

34. Kitagawa M, Aonuma M, Lee SH, Fukutake S, McCormick F. E2F-1 transcriptional activity is a critical determinant of Mdm2 antagonist-induced apoptosis in human tumor cell lines. Oncogene. 2008;27:5303–14.

35. Tovar C, Rosinski J, Filipovic Z, Higgins B, Kolinsky K, Hilton H, et al. Small-molecule MDM2 antagonists reveal aberrant p53 signaling in cancer: implications for therapy. Proc Natl Acad Sci USA. 2006;103:1888–93.

36. Lowe SW, Ruley HE, Jacks T, Housman DE. p53-dependent apoptosis modulates the cytotoxicity of anticancer agents. Cell. 1993;74:957–67.

37. Hayflick L, Moorhead PS. The serial cultivation of human diploid cell strains. Exp Cell Res. 1961;25:585–621.

38. Coppe JP, Desprez PY, Krtolica A, Campisi J. The senescence-associated secretory phenotype: the dark side of tumor suppression. Annu Rev Pathol. 2010;5:99–118.

39. Althubiti M, Lezina L, Carrera S, Jukes-Jones R, Giblett SM, Antonov A, et al. Characterization of novel markers of senescence and their prognostic potential in cancer. Cell Death Dis. 2014;5:e1528.

40. Blasi F, Carmeliet P. uPAR: a versatile signalling orchestrator. Nat Rev Mol Cell Biol. 2002;3:932–43.

41. Jacks T, Remington L, Williams BO, Schmitt EM, Halachmi S, Bronson RT, et al. Tumor spectrum analysis in p53-mutant mice. Curr Biol. 1994;4:1–7.

COMPETING INTERESTS
The authors declare no competing interests.

ETHICS APPROVAL AND CONSENT TO PARTICIPATE
All animal experiments were conducted with the approval of the WEHI Animal Ethics Committee following the guidelines set out by the National Health and Medical Research Council (NHMRC).

ADDITIONAL INFORMATION
Supplementary information The online version contains supplementary material available at https://doi.org/10.1038/s41418-022-00964-7.

Correspondence and requests for materials should be addressed to Andreas Strasser.

Reprints and permission information is available at http://www.nature.com/reprints

Publisher's note Springer Nature remains neutral with regard to jurisdictional claims in published maps and institutional affiliations.